Electronic Supplementary Material (ESI) for Chemical Science.

SUPPLEMENTARY INFORMATION

Dynamical inversion of the energy landscape promotes non-equilibrium self-assembly of binary mixtures

Luis Ruiz Pestana, Natalie Minnetian, Laura Nielsen Lammers, Teresa Head-Gordon

Analysis of diffusive systems. In this section of the SI we analyze the aggregation behavior of diffusive systems where $\Delta A/B \rightarrow \infty$ with three different occupancy densities $\rho = 0.3, 0.5, 0.7$. In all cases, K particles are identical to Cs particles and there is no dependence of the activation barriers on the local environment. Representative snapshots of each system are shown in Figure S1.

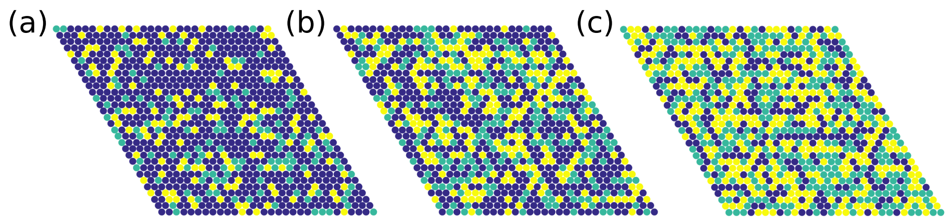

Figure S1. *Snapshots of diffusive systems with occupancy densities. (a) 0.3. (b) 0.5. (c) 0.7.*

Figure S2 shows the scaling of the density fluctuations for the diffusive systems (analogous to Figure 2 in the main text). The results follow closely the scaling expected for equilibrium fluctuations, $\Delta N \sim {N_0}^{0.5}$.

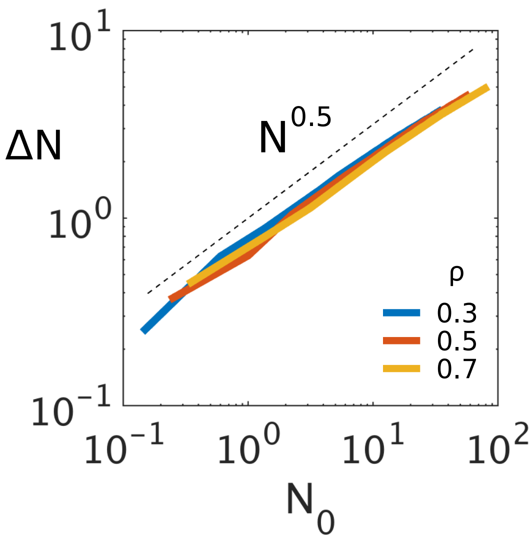

Figure S2. *Fluctuations of the number of particles in diffusive systems.* The results shown are for different occupancy densities. We partition the system into M subsystems of equal size $N_0 = N_{tot}/M$, where N_{tot} is the total number of particles in the system. Each time step, for each subsystem, we calculate $\Delta N(t) = N(t) - N_0$. (a) Average of the fluctuations over time and over all the subsystems, ΔN, as a function of the reference number of particles per subsystem, N_0. The black dashed line shows the scaling of equilibrium $\Delta N \sim N^{0.5}$.

The values of $\langle f^i_{agg} \rangle$ shown in Figure 4 in the main text are corrected from the background aggregation due to equilibrium density fluctuations shown here in Figure S2b. Figure S2a shows the probability distributions of f^{Cs}_{agg}. The results for K are analogous, and are not shown. Lastly, Figure 2c shows the power spectrum of f_{agg}^{Cs} (analogous to Figure 5 in the main text). The diffusive systems exhibit an approximately horizontal spectrum, characteristic of white noise, in clear contrast to cases with finite values of $\Delta A/B$, where pink noise is observed instead (Fig. 5).

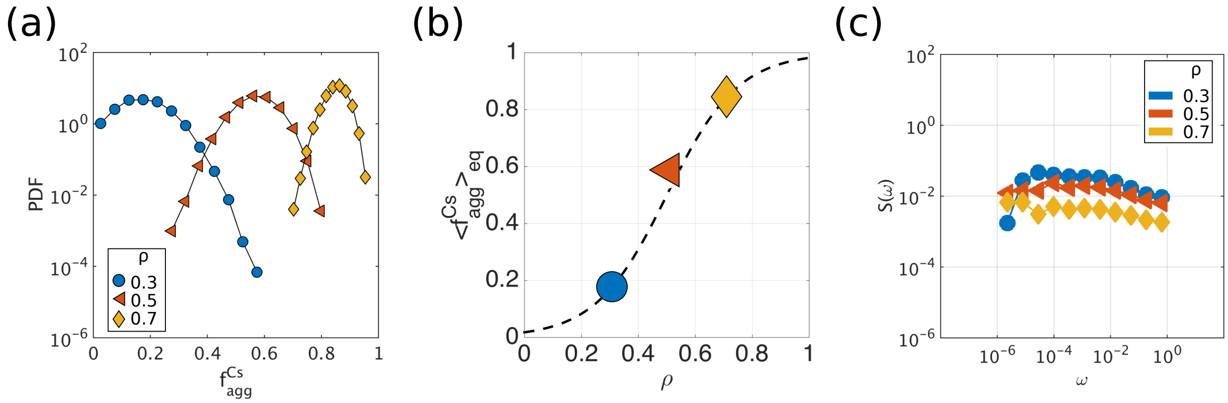

Figure S3. *Aggregation behavior of the diffusive systems.* (a) Probability distributions of the aggregation fraction, f_{agg}^{Cs}. (b) Average aggregation fraction, $\langle f_{agg}^{Cs} \rangle$, as a function of ρ. The dashed black line is a fit of a sigmoidal function to the data, $\langle f_{agg}^{Cs} \rangle = \left[1 + e^{8(\rho-0.5)}\right]^{-1}$. (c) Power spectrum of the fluctuations of f_{agg}^{Cs}.

Sensitivity to initial conditions. While the results report initial conditions of a well-mixed system, we show that the system that starts from a phase separated configuration also exhibits the DIEL phenomena. In Figure S4 we see that there is an initial transient period where Cs (yellow) forms a cohesive front kinetically trapping the K particles (cyan) in one of the reflective boundaries (i.e. left or right), and illustrated in frames 45,000 and 120,000. Once the system escapes this transient state via a finite size fluctuation in the compact Cs front, the system resumes it's corresponding cyclic behavior with micelle-like cluster formation as reported in the paper. At long times, we find the same behavior starting from a well mixed or a phase separated configuration.

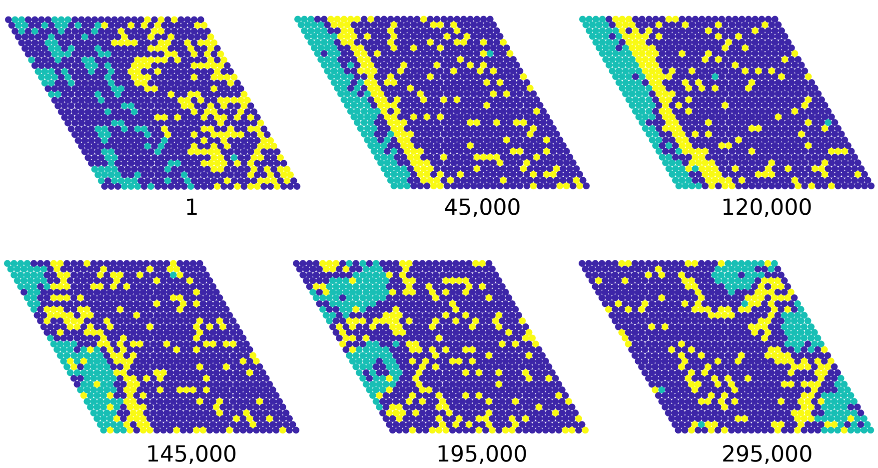

Figure S4. Sequence of snapshots in a 30x30 lattice sites system starting from phase separated configurations. The numbers underneath are the frames of the simulation where the snapshot was taken. In these simulation B = 23 and ΔA=16.

Additional analysis on systems with finite values of ΔA/B

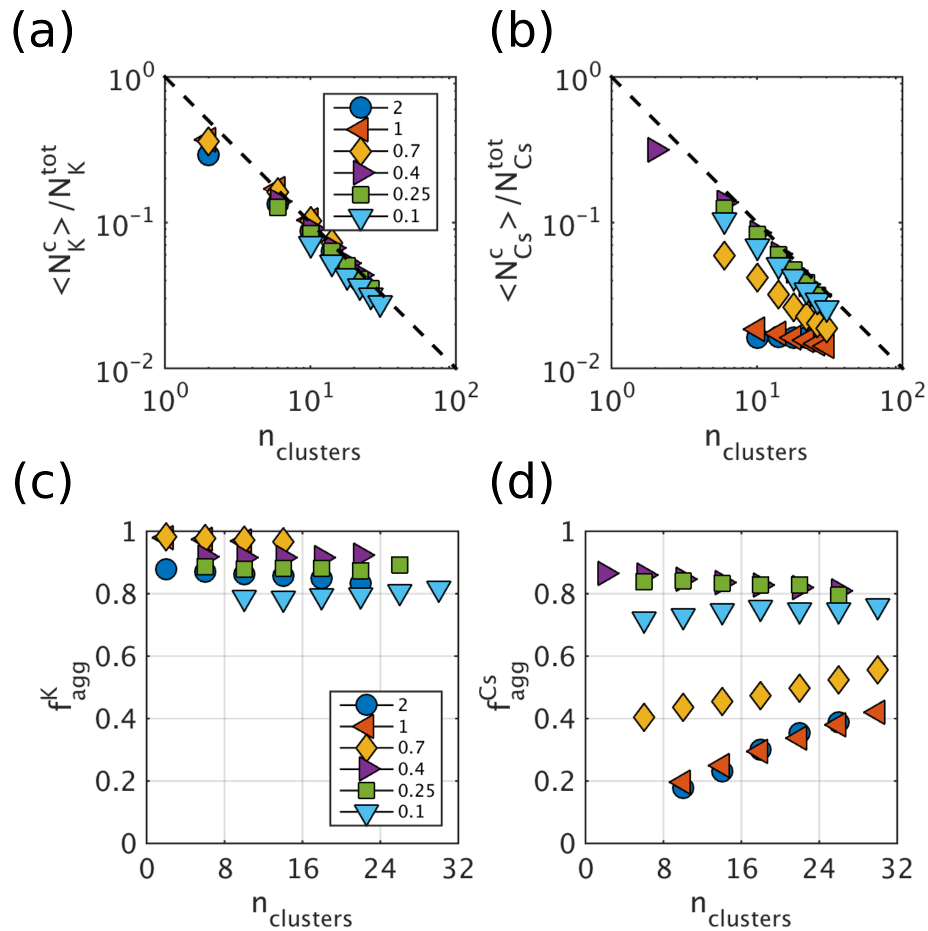

Figure S5. *Clustering behavior.* Panels (a) and (b) show the normalized average cluster size, $\langle N_K{}^c \rangle / N_K{}^{tot}$, as a function of the instantaneous number of clusters, $n_{clusters}$, for K and Cs respectively. The axes are logarithmic, and the dashed lines correspond to $\langle N_K{}^c \rangle / N_K{}^{tot} = n_{clusters}{}^{-1}$. Panels (c) and (d) show the aggregation fraction as a function of the number of clusters for K and Cs respectively. The results shown in the figure are for $\rho = 0.3$.

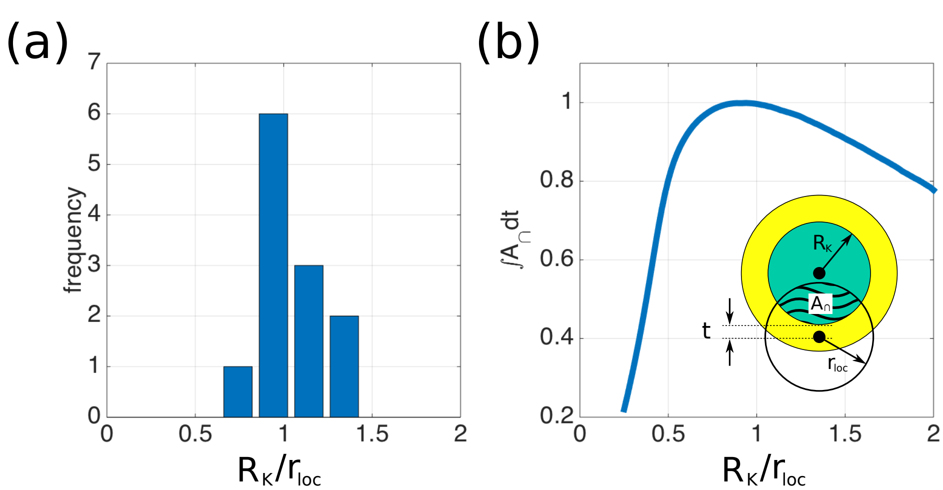

Figure S6. *Analysis of the core cluster size, R_K, in relation to the characteristic length scale of the local environment, r_{loc}.* (a) Histogram of the average R_K, normalized by the characteristic size of the local environment, r_{loc}. The data is collected from simulations where $r_{loc} = 4$. (b) Total overlap area between the local environment of Cs particles in the corona and the K particles in the core, as a function of R_K / r_{loc}.